Fast data assimilation for open channel hydrodynamic models using control theory approach

Miloš Milašinović[1*], Dušan Prodanović[2], Budo Zindović[3], Nikola Rosić[4], Nikola Milivojević[5]

[1]University of Belgrade, Faculty of Civil Engineering, Department of Hydraulic and environmental engineering, Bulevar Kralja Aleksandra, mmilasinovic@grf.bg.ac.rs

[2]University of Belgrade, Faculty of Civil Engineering, Department of Hydraulic and environmental engineering, Bulevar Kralja Aleksandra, dprodanovic@grf.bg.ac.rs

[3]University of Belgrade, Faculty of Civil Engineering, Department of Hydraulic and environmental engineering, Bulevar Kralja Aleksandra, bzindovic@grf.bg.ac.rs

[4]University of Belgrade, Faculty of Civil Engineering, Department of Hydraulic and environmental engineering, Bulevar Kralja Aleksandra, nrosic@grf.bg.ac.rs

[5]Jaroslav Černi Water Institute, Belgrade, nikola.milivojevic@jcerni.rs

*Corresponding author

Abstract: Model-driven forecasting, used for flood risks or big hydropower systems management, can produce results of unsatisfying accuracy even with best-calibrated hydrodynamic models. One of the biggest uncertainty sources is the inflow data, either produced by different hydrological models or obtained using unreliable rating curves. To keep the model in the up-to-date state, data assimilation techniques are used. The aim of the assimilation is to reduce the difference between simulated and observed state of selected variables by updating hydrodynamic model state variables according to observed water levels. The widely used data assimilation method applicable for nonlinear hydrodynamic models is Ensemble Kalman Filter (EnKF). However, this method can often increase the computational time due to complexity of mathematical apparatus, making it less applicable in everyday operations. This paper presents the novel, fast, tailor-made data assimilation method, suitable for 1D open channel hydraulic models, based on control theory. Using Proportional-Integrative-Derivative (PID) controllers, the difference between measured levels

and simulated levels obtained by hydrodynamic model is reduced by adding or subtracting the flows in the junctions/sections where water levels are measured. The novel PID control-based data assimilation (PID-DA) is compared to EnKF. Benchmarking shows that PID-DA can be used for data assimilation, even coupled with simplified 1D hydraulic models, without significant sacrifice of stability and accuracy, and with reduction of computational time up to 63 times.

Keywords: *PID control; control loop feedback mechanism; short-term forecasting; Ensemble Kalman filter; data assimilation speed up*

1. INTRODUCTION

Population growth and high urbanization under ongoing climate changes have created society highly sensitive to increasingly frequent extreme hydrological events (Coumou and Rahmstorf 2012; IPCC 2012). Managing flood risks and river systems used for electrical energy production, water supply, irrigation or inland navigation, even in regular, average hydrological events, and especially during extremes, creates extra pressure in decision-making. In order to optimize the water resources management on daily basis, experts require long-term and, more often, short-term forecasts. For this purpose, different numerical models and monitoring systems are used.

The quality of model-driven forecast (e.g. water level forecasting) is often reduced due to numerous uncertainty sources (Bozzi et al. 2015; Vrugt et al. 2008). Inflows are susceptible to uncertainties (as analyzed by Bai *et al.*, 2016) mostly due to high uncertainty of rating curves (Ocio *et al.* 2017) or inadequate hydrological model used. Additionally, model calibration is done only for selected (historical) sets of data. This results in model's inability to produce results of satisfying accuracy when simulating current real-life conditions. In order to overcome this and improve model's simulation accuracy, Data Assimilation (DA) techniques are widely used (Vrugt et al. 2006).

DA combines results from previously calibrated model with observation (measured) data, together with model's and observation's uncertainties, and computes the update of model's

54 state, dynamically reducing model's uncertainty and providing better forecasts (Habert et al.
55 2016). Different DA tools have been successfully applied in hydrological and hydrodynamic
56 modelling. One of the most commonly used is Kalman filter (Kalman 1960) and its
57 modifications used for highly nonlinear models (Evensen 2003), named Ensemble Kalman
58 Filter (EnKF) (Reichle et al. 2002). Madsen *et al.* (2003) applied EnKF coupled with MIKE 11
59 hydrodynamic model to improve the flood forecast in the Piedmont region in the northwestern
60 part of Italy. Vrugt *et al.* (2006) used the Sacramento Soil Moisture Accounting conceptual
61 watershed model (SAC-SMA) coupled with EnKF for operational streamflow forecasting and
62 flood warning systems in the USA. Coupling hydrological model and EnKF algorithm was
63 also presented in Clark *et al.* (2008), where streamflow observations were used in order to
64 update states (water levels). Coupling EnKF and hydrodynamic model based on shallow
65 water Saint-Venant's equations increased forecast accuracy of 50-70% as presented by
66 Neal, Atkinson and Hutton (2007). Combination of LISFLOOD-FP (Bates and Roo 2000) and
67 EnKF was presented in Andreadis *et al.* (2007), Andreadis and Schumann (2014) and
68 Munier *et al.* (2014). Neal *et al.* (2009) applied EnKF in combination with HEC-RAS model
69 (Brunner 2010) in order to estimate river discharge on an un-gauged basin using water level
70 data obtained by satellite images. Application of Synthetic-Aperture-Radar images for
71 assimilation into hydraulic models was presented in several researches (García-Pintado et
72 al. 2013; Mason et al. 2012). Recent research in the area of DA for flood forecast on big
73 rivers was done by Barthélémy *et al.*, (2017), using EnKF coupled with MASCARET
74 hydraulic model (Goutal and Maurel 2002) for operational flood forecasting on the Adour
75 Maritime river. Further analyses of observations and parameters impact and domain length
76 for flood forecasting can be found in Cooper *et al.*, 2018.

77 All these researches show high applicability of EnKF in hydrologic/hydraulic modelling. Even
78 though the EnKF is the most commonly used DA method it has some restrictions. In order to
79 avoid those restrictions, some more complex methods are used: Particle Filters (presented
80 by Del Moral (1997)) (Chen, Pang, and Wu 2018; Matgen et al. 2010; Moradkhani et al.
81 2005; Xu et al. 2017), variational methods (Kabir, Appiah Assumaning, and Chang 2017; Seo

et al. 2009) or new method called Ensemble Smoother (Li, Stetler, et al. 2018; Li, Puzel, and Davis 2018).

The main drawback of EnKF and all other complex methods is that they are computationally expensive. When used for hydrological/hydraulic forecast, in many cases those methods will fail to perform in reasonable time (Madsen and Skotner 2005). If there is requirement for fast evaluation and forecast of the water system state, in order to prevent or reduce flood hazards and/or increase benefit from hydropower production, then there is necessity for easy understanding and time effective modelling/assimilation tool for everyday use by water system operators. Many researchers tried to develop simplified, tailor-made, assimilation techniques suitable for solving some specific problems. For example, Madsen and Skotner (2005) developed a cost-effective filtering procedure for river model. Instead of computing Kalman gain matrix for each assimilation step, the procedure uses the predefined set of gains to update the water levels. On the other hand, Hansen *et al.*, (2014) applied deterministic water level assimilation in urban drainage systems for better flow forecast. This approach, presented by Hansen *et al.* (2014), uses indirect water level update, based on adding/subtracting correction flow to the system.

This paper presents DA methodology based on adding/subtracting correction flows at observation locations. In this research, correction flows are calculated using Proportional-Integrative-Derivative (PID) controllers in the procedure called PID control-based data assimilation (PID-DA). The PID-DA is developed for 1D open channel hydraulic models, used for modelling river systems, where correction flows are implemented as simple lateral (fictive) inflow in continuity equation. Potential of using the PID controllers as DA tool was introduced in Rosić, Jaćimović, et al. (2017) and in Rosić, Prodanović, et al. (2017), providing just the general overview of the methodology and without comparing with the existing DA techniques. Milasinovic et al. (2018), (2019) continued developing and testing PID-DA but without benchmarking with other DA methods and without analysis of time cost efficiency. Therefore, this paper presents further insight into the novel DA methodology (PID-DA).

The aim of this paper is to present and test the novel, tailor-made, PID-DA approach. The paper will benchmark PID-DA to the EnKF, showing that this novel approach is easy to implement in 1D hydraulic models, is fast and robust. PID-DA and EnKF are applied for correction of model states (water levels) in the assimilation window (period when observations are available) on test examples. Along with water level assimilation performance assessment, computational efficiency is also compared. Different PID controllers and EnKF settings are applied to hydraulic (hydrodynamic) models of different complexity. The analysis presented in the paper shows that PID controllers as DA tool can be coupled with simplified hydraulic model, without significant sacrifice of accuracy. The main benefit of using PID-DA is substantial reduction of computational time and ease of implementation, which often limits the application of EnKF in everyday water systems operations.

2. METHODS AND MATERIALS

2.1. Methodology overview

Formal DA procedure (EnKF, PF, variational methods, etc.) can be described using two repeating steps. In the first step, ***forecast***, the (river) model is used in free-run mode to calculate the variables describing the system state (water levels) using several calculation time steps with known model's driving data (inflows). Next step of data assimilation process is ***correction*** of the forecasted states (correction of levels) at the present (or current) time, when observations (level measurements with assessed uncertainty) are available, Fig. 1a. Correction of the states is conducted according to the selected assimilation algorithm (EnKF, PF) and uncertainties of both measured and forecasted levels. Since correction of present model's state is done, it is named in this paper as Real-Time assimilation (RTa), regardless of time spent in the EnKF or PF algorithm. If observations are not available at the current time, no correction is performed.

Novel DA tool in 1D open channel hydraulic model (PID-DA) requires slight modification of formal data assimilation procedure. The assimilation is not Real-Time (RTa) in a sense that

just one, current observation is used to correct present state of the model. Assimilation is done in a Near Real-Time (NRTa), for selected previous period, when measurements already exist. During that previous period, model is ***continuously updated*** in each simulation time step, using either measured or interpolated water level data in order to reduce the difference between measurements and model results (Fig. 1b). The assumption in presented procedure is that inflow data are with much higher uncertainty than measured water levels. Hence, PID controllers will add/remove flow from the model to reduce difference between modelled and measured water levels. Having this assumption extends to the assumption that main source of uncertainty are non-reliable boundary conditions (e.g. unreliable data for upstream or lateral inflows obtained by hydrological models, unreliable rating curves, etc.). The model update is controlled by several PID controllers which continuously add/remove the flows at assimilation locations (at selected observation locations, using fictive lateral inflow). Flows, added or subtracted at assimilation locations, are calculated using Proportional-Integrative part of the controller, according to water level difference between observed (measured) and calculated levels. A PID controller (Karl Astrom 2002; Skogestad 2004) is a control loop feedback mechanism that adjusts the added flow, trying to reduce the water level difference in a reasonable time.

Because of the continuous PID controller's nature, forecast and correction steps are not clearly divided. The correction is conducted at each computation time step, during the selected, previous period of simulation process (Fig. 1b). Since time step for measured data is much longer than computation time step, the water level difference is computed based on the linear interpolation between measured levels ("Interpolated state used for NRTa" on Fig. 1b).

The explanation of PID-DA for 1D hydraulic model is presented in the following sections. General application of PID controller-based data assimilation on river model is presented in the Figure 2.

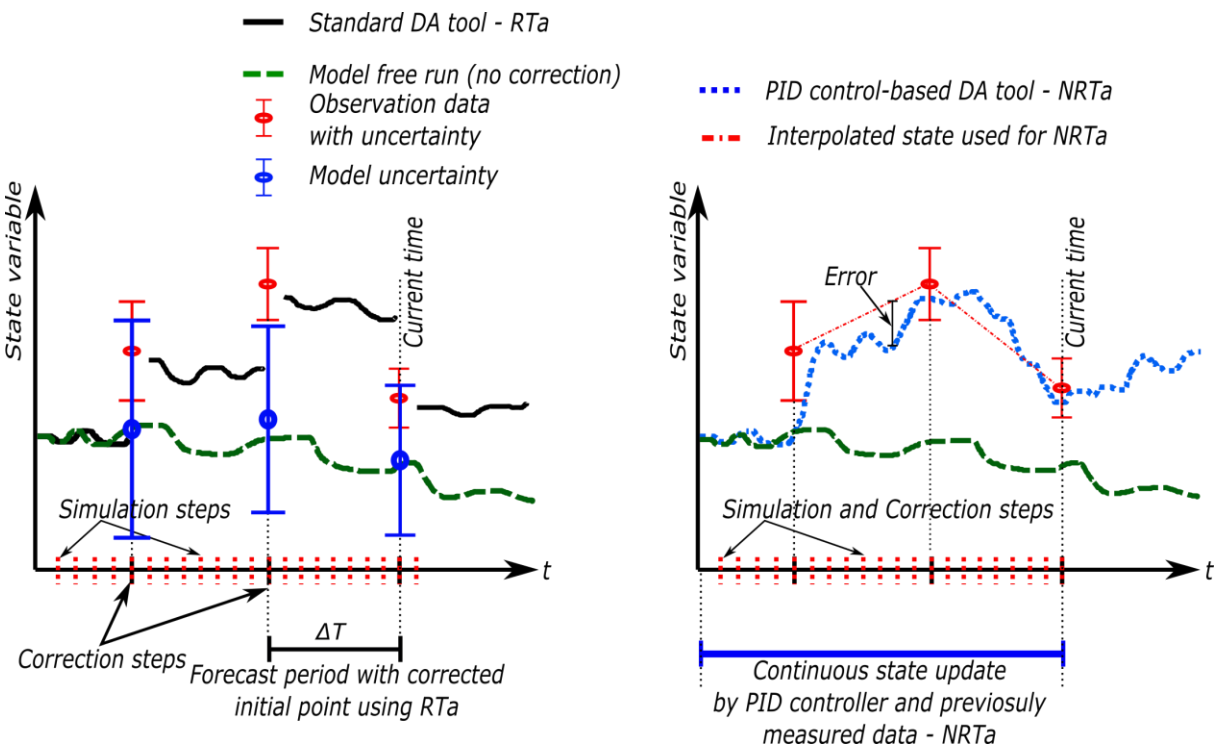

a) b)

Figure 1. General data assimilation procedure. a) standard EnKF, b) with PID controller

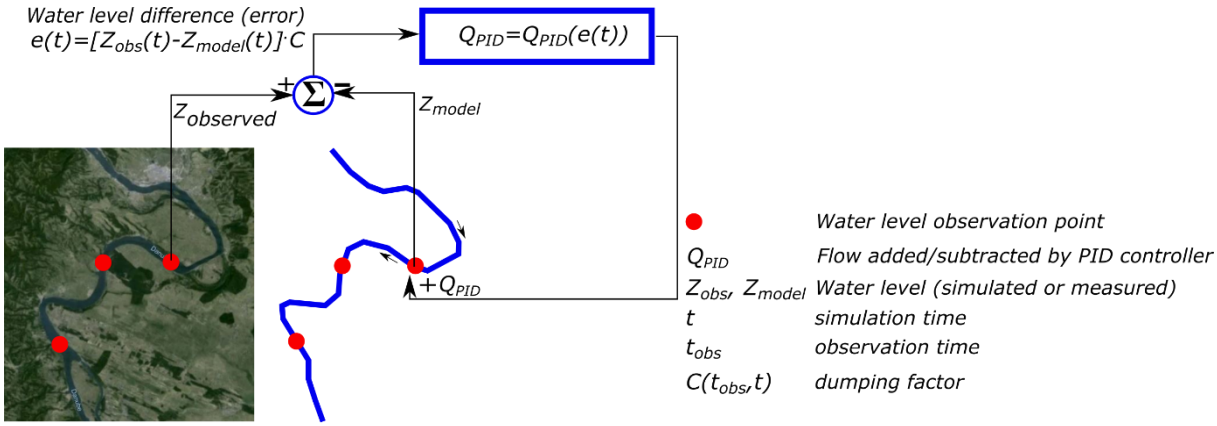

Figure 2. PID controller-based data assimilation procedure for water level updating in 1D hydrodynamic models (example: Danube section downstream of Iron Gate, border between Serbia and Romania)

2.2. 1D hydrodynamic diffusion wave model – DiffW1D

To analyze the effects of model's complexity on both PID-DA and EnKF, diffusion wave model is used. This model for water level forecasting is based on 1D Saint-Venant equations (1) and (2) (Costabile and Macchione 2012)). Diffusion wave model is derived from the full

Saint-Venants equations by neglecting convective acceleration in momentum conservation equation (2).

$$\frac{\partial A}{\partial t}+\frac{\partial Q}{\partial x}=q \tag{1}$$

$$\frac{\partial Q}{\partial t}+\frac{\partial}{\partial t}\left(\beta\frac{Q^2}{A}\right)+gA\frac{\partial Z}{\partial x}+gn^2\frac{Q|Q|}{A^2\cdot R^{4/3}}=0 \tag{2}$$

Original diffusion wave model neglects inertial terms in eq. (2) (first and the second terms). Diffusion wave model implemented in this paper (DiffW1D) differs from the original form by adding local acceleration term ($\partial Q/\partial t$) including the backward wave propagation effect (Petrovic, Palmar, and Ivetic 1994). Model domain discretization is presented in Fig. 3a. Using this approach, river domain is divided by cross-sections. Numerical DiffW1D model use staggered numerical scheme where water levels and flows are calculated in alternating cross-sections (Abbot and Basco 1989) as presented in the Fig. 3b. Numerical model of the diffusion wave is given by the equations (3) and (4):

$$Z_i^{t+\Delta t}=Z_i^t-\frac{\Delta t}{B_i^t}\cdot\frac{Q_{i+1}^t-Q_{i-1}^t}{2\Delta x} \tag{3}$$

$$Q_{i+1}^{t+\Delta t}=\frac{\dfrac{Q_{i+1}^t}{g\left(\dfrac{A_{i+2}^{t+\Delta t}+A_i^{t+\Delta t}}{2}\right)\Delta t}-\dfrac{Z_{i+2}^{t+\Delta t}-Z_i^{t+\Delta t}}{2\Delta x}}{\dfrac{1}{g\left(\dfrac{A_{i+2}^{t+\Delta t}+A_i^{t+\Delta t}}{2}\right)\Delta t}+\dfrac{n^2}{\left(\dfrac{A_{i+2}^{t+\Delta t}+A_i^{t+\Delta t}}{2}\right)^2\left(\dfrac{R_{i+2}^{t+\Delta t}+R_i^{t+\Delta t}}{2}\right)^{4/3}}\cdot\left|Q_{i+1}^t\right|} \tag{4}$$

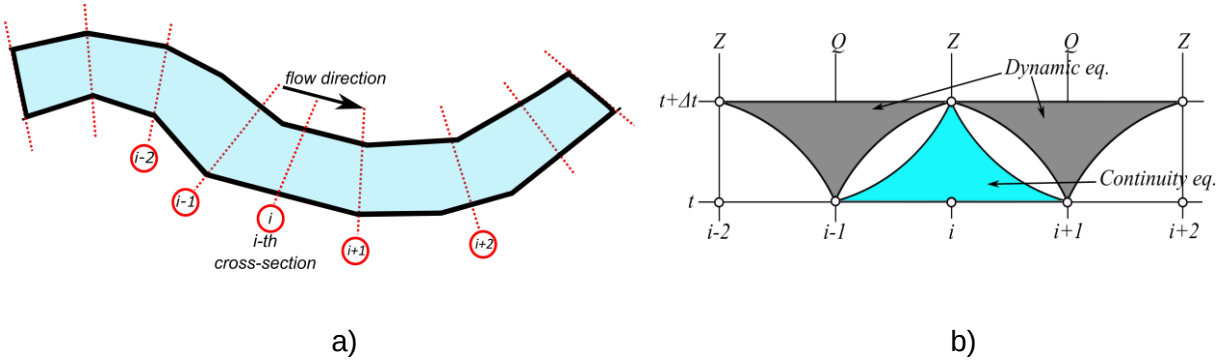

a) b)

Figure 3. (a) Model domain discretization and (b) numerical scheme using DiffW1D model

Numerical model analyzed in this paper, together with used assimilation algorithms, is coded in MATLAB (MathWorks Inc. 2018). Computational time is measured only for the part of the code where the model equations and assimilation are performed; pre-processing and post-processing phase were not included in simulation efficiency tests.

2.3. Assimilation methods

Well established EnKF data assimilation is used as benchmark to assess the performance of the new PID control-based algorithm. PID controller-based assimilation is developed under the assumption that the main source of uncertainty in the model is the inflow as boundary condition.

2.3.1. PID control-based data assimilation – PID-DA

Proportional-Derivative-Integrative controller is a control loop feedback mechanism, where input in the next step is a function of the previous output (Karl Astrom 2002). This mechanism is often used for Real-Time-Control of different process (e.g. RTC of hydraulic structures in urban drainage systems (Schütze et al. 2004)). PID controller input is named as *error*, which is calculated as a difference between current value of the *process variable* (e.g. water level) and the *setpoint* of the variable (e.g. desired water level). PID controller tends to reduce *error* using the *control variable*. When PID controller is applied as data assimilation tool (PID-DA), error $e(t)$ is calculated as difference between observed water level $Z_{obs}(t)$ and water level obtained by 1D hydraulic model $Z_{model}(t)$. Control variable used to reduce this error is lateral inflow $Q_{PID}(t)$ (Fig. 2, eqs. (5) and (6)).

$$Q_{PID}(t) = Q_{PID}^{t} = P \cdot e(t) + I \cdot \int_{t_0}^{t} e(t)dt + D\frac{d(e)}{dt} \tag{5}$$

$$e(t) = Z_{obs}(t) - Z_{model}(t) \tag{6}$$

PID parameters are: P - proportional gain factor used to multiply the current error value, I - integrative gain factor used to add the influence of previous errors and D - derivative gain

206 factor used to adopt control to current trends in error change. Mostly, PID controller is used
207 as the Proportional (*P*) or Proportional-Integrative (*PI*) controller. Goal of PID control is to
208 reach setpoint in a system in reasonable time (reach the measured water levels by adjusting
209 the model). *P* gain produces an output based only on the current value of the error. High
210 values of *P* gain cause big variations in controllers' output that can make system unstable
211 (extremely big correction flow in one time step, extremely low correction flow in the next time
212 step). Low values (towards zero) of *P* gain avoid problems of unstable system, but time
213 needed for reaching the setpoint increases and, practically, makes system unable to reach
214 the goal. Therefore, integrative *I* gain is used. This gain collects previous errors and their
215 duration, trying to minimize them over time. This gain can significantly reduce time needed
216 for reaching the setpoint. In some cases, in highly dynamical systems with rapid changes,
217 Derivative component is included to estimate the error trend (what will be the error in the
218 near future). However, the *D* component is sensitive in systems with high measurement
219 noise and can enhance the controller's instability. Hence, proper tuning of the parameters
220 depends on the problem being solved (there are no recommended values). Tuning the P, I
221 and D gains can be done manually (by trial and error) or using some heuristic approaches
222 (Ziegler and Nichols 1995).

223 Original form of the error calculation (difference between value of process variable and
224 setpoint) given by the eq. (6), assumes that observation time step Δt_{obs} is equal to the
225 simulation time step Δt. In most applications, the simulation time step is much shorter and, in
226 the period between two existing observations, the "observed" state in eq. (7) is calculated
227 using linear interpolation. It can be assumed that the accuracy of interpolated "observed"
228 level is decreasing as the time interval from the last observation is increasing, so a form of
229 dumping factor is introduced. In this paper, it is defined by eq. (8) and is presented on Fig. 4.

$$e(t) = \left[Z^{*}_{obs}(t) - Z_{\mathrm{mod}el}(t) \right] \cdot C \tag{7}$$

$$C = \begin{cases} 1 & t = t_{obs} \\ \dfrac{\Delta t_{obs}}{t + \Delta t_{obs} - t_{prev\_obs}} & t \neq t_{obs} \end{cases} \quad (8)$$

230

231 In eq. (7), Z^*_{obs} represents observed water levels obtained by linear interpolation, Z_{model} is
232 simulated water level and C is dumping factor. In eq. (8) t_{prev_obs} is time of the previous
233 available observation, t is current simulation time, t_{obs} is observation time and Δt_{obs} is
234 observation time step.

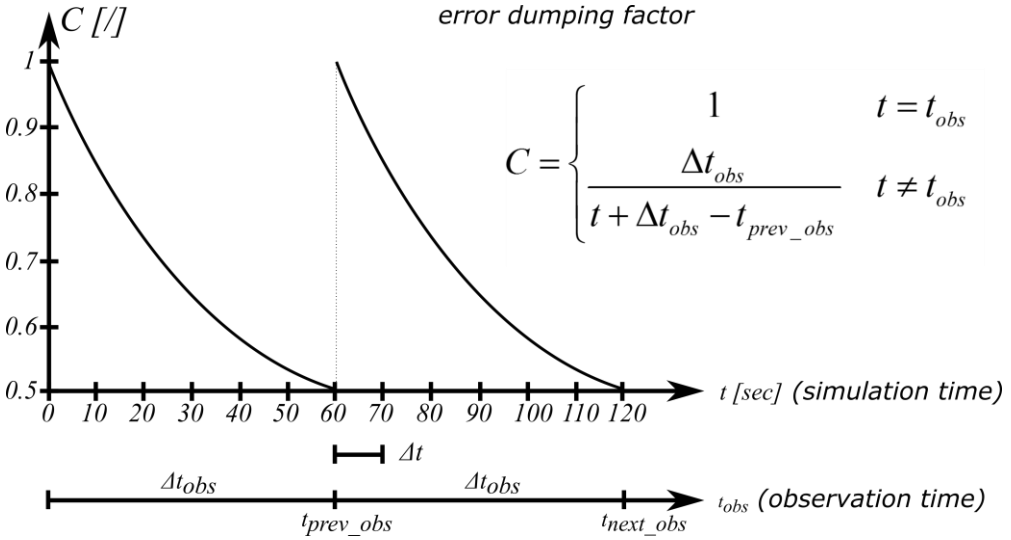

235

236 Figure 4. Error dumping factor (periodical, discontinuous, function) as measure of uncertainty
237 (minimal value of the dumping factor depends on specific values of simulation time step Δt
238 and observation time step Δt_{obs})

239 Dumping factor in eq. (7), will gradually turn off PID controller (Fig. 4) in periods between two
240 measurements. This means that, as model progress forward in time, in period without
241 measurements, smaller weight is given to the errors calculated using interpolated water
242 levels. Dumping function can be also seen as a way to include the observation uncertainty
243 into the process of assimilation: the error function for measurements with higher uncertainty
244 will be smaller, reducing the influence of measurement over the simulation. Using data
245 quality evaluation algorithm in a pre-processing phase (e.g. N. Branisavljević, Prodanović,
246 and Pavlović (2010) and Branisavljević, Kapelan, and Prodanović (2011)) the value of
247 dumping function can be estimated. This means that if data quality, assessed through one of

248 the data quality algorithms, is low, smaller weights would be given to the errors calculated
249 using this data. Another multiplier in eq. (7) would be used for implementation of this type of
250 dumping factor. In this research, only dumping factor for reducing impact of interpolated
251 water levels is used. Thus, in used PID-DA algorithm, only observation uncertainty is
252 included, unlike EnKF data assimilation where both model's and observation's uncertainties
253 are used.

254 PID controllers are implemented as lateral inflow elements in hydraulic model. Therefore, eq.
255 (3) used in DiffW1D model has the following shape:

$$Z_i^{t+\Delta t} = Z_i^t - \frac{\Delta t}{B_i^t} \cdot \frac{Q_{i+1}^t - Q_{i-1}^t}{2\Delta x} + \frac{\Delta t}{B_i^t} \frac{Q_{PID}^t}{2\Delta x} \tag{9}$$

256 2.3.2. Ensemble Kalman filter (EnKF) with SLS inflation and localization

257 Ensemble Kalman Filter – EnKF (Evensen 1994, 2003) is used for benchmarking the
258 proposed PID-DA method. EnKF algorithm implemented in this paper is used for state
259 estimation, where water levels in each discretization element (reservoir or cross-section) are
260 considered as model state variable. In order to use EnKF algorithm for data assimilation,
261 state vector $\mathbf{X} = [x_i],\ (i = 1, 2, ..., N_{sv})$ has to be defined, where x_i represents water levels at i^{th}
262 cross-section, and N_{sv} is the number of state variables in the model. When EnKF is used,
263 model uncertainty estimation is conducted through ensemble statistics, where each element
264 of the state vector **X** is represented by ensemble created by adding Gaussian noise to the
265 previous values of state vector variables. In this paper, 50, 100 and 200 ensemble members
266 are analyzed.

267 State of the vector **X** after each time step is calculated using the following equation:

$$\mathbf{X}^{t+\Delta t} = \mathbf{X}_e^{t+\Delta t} + \left[\mathbf{K}_\mathbf{X} \cdot \left(\mathbf{Y} - \mathbf{H} \cdot \mathbf{X}_e^{t+\Delta t}\right)\right] \tag{10}$$

268 Where t denotes previous time and $t+\Delta t$ denotes current time. Index e (in $\mathbf{X}_e^{t+\Delta t}$) indicates
269 that this is evaluated state vector based on model only. This state vector is corrected using
270 the Kalman gain $\mathbf{K_X}$, and measured data **Y**. **H** matrix represents mapping operator used for

mapping observation locations with matching variables in the state vector $\mathbf{X}$. Definition of the **H** matrix is presented in Fig. 5.

Kalman gain **Kx** is calculated using the following equation:

$$\mathbf{K}_{\mathbf{X}} = \mathbf{P} \cdot \mathbf{H}^T \cdot \left(\mathbf{H} \cdot \mathbf{P} \cdot \mathbf{H}^T + \mathbf{B}_{obs} \right)^{-1} \tag{11}$$

Where **P** is model error covariance matrix and $\mathbf{B}_{obs}$ is observation error covariance matrix. Procedure for calculation of **P** and $\mathbf{B}_{obs}$ can be seen in Evensen (1994) and (2003).

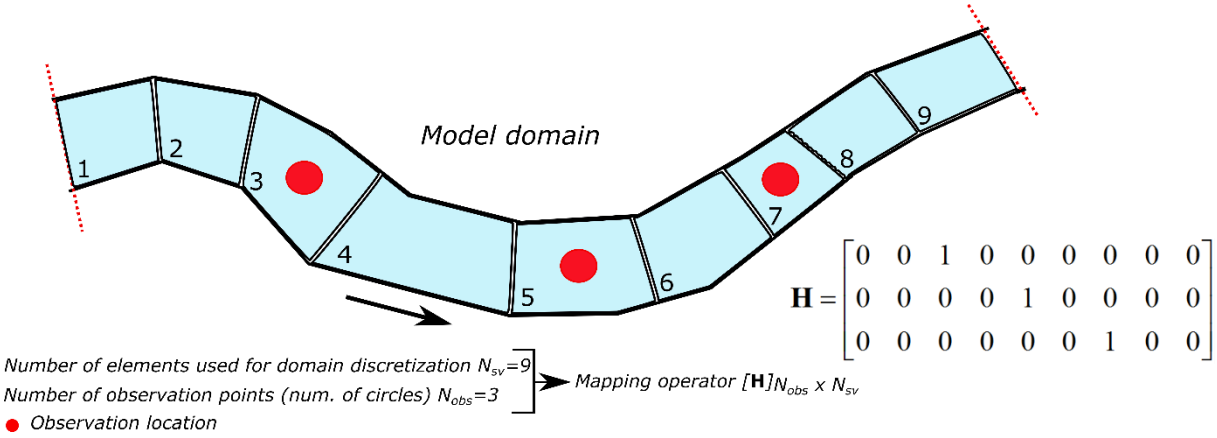

Figure 5. Mapping operator **H** definition

Limitation of the ensemble size can affect filter performance and create divergent filter where observed data are ignored over time. One of the reasons causing this problem is the presence of spurious correlations evaluated in model error covariance matrix. Therefore, different methods for eliminating this problem have been developed. Most common methods used for eliminating this problem are inflation methods where model error covariances are increased in order to prevent filter divergence (Anderson 2007; Anderson and Anderson 1999). Wu and Zheng, 2018 presented Second-order Least Square (SLS) inflation scheme, which is applied in this paper. First step in SLS inflation scheme is to calculate forecasted residuals **d** by the eq. (12).

$$\mathbf{d} = \mathbf{Y} - \mathbf{H} \cdot \mathbf{X}_e^{t+\Delta t} \tag{12}$$

When residuals are evaluated, inflation factors λ (model error covariance inflation factor) and μ (observation error covariance inflation factor) are calculated using the following equations:

$$\lambda = \frac{Tr\left(\mathbf{d}^T\mathbf{HPH}^T\mathbf{d}\right)\cdot Tr\left(\mathbf{B}_{obs}^2\right) - Tr\left(\mathbf{d}^T\mathbf{B}_{obs}\mathbf{d}\right)\cdot Tr\left(\mathbf{HPH}^T\mathbf{B}_{obs}\right)}{Tr\left(\mathbf{HPH}^T\mathbf{HPH}^T\right)\cdot Tr\left(\mathbf{B}_{obs}^2\right) - Tr\left(\mathbf{HPH}^T\mathbf{B}_{obs}\right)^2} \quad (13)$$

$$\mu = \frac{Tr\left(\mathbf{HPH}^T\mathbf{HPH}^T\right)\cdot Tr\left(\mathbf{d}^T\mathbf{B}_{obs}\mathbf{d}\right) - Tr\left(\mathbf{d}^T\mathbf{HPH}^T\mathbf{d}\right)\cdot Tr\left(\mathbf{HPH}^T\mathbf{B}_{obs}\right)}{Tr\left(\mathbf{HPH}^T\mathbf{HPH}^T\right)\cdot Tr\left(\mathbf{B}_{obs}^2\right) - Tr\left(\mathbf{HPH}^T\mathbf{B}_{obs}\right)^2} \quad (14)$$

289 Where Tr denotes trace operator. When inflation factors are evaluated, Kalman gain $\mathbf{K_x}$, eq.
290 (11), is modified (eq. (15)):

$$\mathbf{K}_{\mathbf{x}}^{SLS} = \lambda\cdot\mathbf{P}\cdot\mathbf{H}^T\cdot\left(\mathbf{H}\cdot\lambda\cdot\mathbf{P}\cdot\mathbf{H}^T + \mu\cdot\mathbf{B}_{obs}\right)^{-1} \quad (15)$$

291 The second method commonly used for elimination of EnKF drawbacks mentioned before is
292 localization method (Petrie and Dance 2010). This method modifies model error covariance
293 matrix by eliminating spurious correlations (Hamill, Whitaker, and Snyder 2001; Wang et al.
294 2018). Model error covariance matrix is modified by correlation matrix ρ multiplication.
295 Correlation matrix (Gaspari and Cohn 1999) is calculated by the eq. (16)

$$\rho = \begin{cases} -\frac{1}{4}(l/c)^5 + \frac{1}{2}(l/c)^4 + \frac{5}{8}(l/c)^3 - \frac{5}{3}(l/c)^2 + 1, & 0 \le l \le c \\ \frac{1}{12}(l/c)^5 - \frac{1}{2}(l/c)^4 + \frac{5}{8}(l/c)^3 - \frac{5}{3}(l/c)^2 - 5(l/c) + 4 - \frac{2}{3}(l/c)^{-1}, & c \le l \le 2c \\ 0 & l \ge 2c \end{cases} \quad (16)$$

296 where l is Euclidean distance between either the grid points in physical space or the grid
297 point and the observation location. Here, l represents Euclidean distance between cross-
298 sections used for water level estimation (distance between each two cross-sections used by
299 model). c represents a length scale, such that correlation reduces from 1 when distance l is
300 bigger than c (c can be set to different values, depending on a problem being solved). Hence,
301 ρ is a N_{sv} x N_{sv} correlation matrix. Accordingly, Kalman gain is modified by eq. (17).

$$\mathbf{K}_{\mathbf{x}}^{loc} = \left(\rho\circ\mathbf{P}\right)\cdot\mathbf{H}\cdot\left[\mathbf{H}\cdot\left(\rho\circ\mathbf{P}\right)\cdot\mathbf{H}^T + \mathbf{B}_{obs}\right]^{-1} \quad (17)$$

302 Operator "∘" in eq. (17) denotes Schur product of two matrices.

303 When localization method is used in hydrodynamic modelling, spurious correlations between
304 distant cross-sections or reservoirs (depends on elements used for model domain

discretization) are neglected or reduced, depending on the distance. Practically, this means that changes in one model element (reservoir or cross-section) cannot immediately cause changes in distant elements (these changes in distant areas can be seen after certain amount of time needed for change propagation). Therefore, length scale c is used for limiting the number of model elements affected by changes caused by assimilation process in assimilation points according eq. (17). If localization is not used, each correction step will induce changes in all model elements at the same time, which can induce model instabilities (big oscillations of water levels with high amplitude).

Modification of the Kalman gain used in this paper combines both methods, inflation and localization (eqs. (15) and (17)). Hence, Kalman gain modification is given by the following equation (18).

$$\mathbf{K}_{\mathbf{X}} = \lambda \cdot (\rho \circ \mathbf{P}) \cdot \mathbf{H} \cdot \left[\lambda \cdot \mathbf{H} \cdot (\rho \circ \mathbf{P}) \cdot \mathbf{H}^T + \mu \cdot \mathbf{B}_{obs} \right]^{-1} \tag{18}$$

2.4. Test cases

Proposed PID-DA is compared with EnKF method on two hypothetical test cases with different complexity of cross section geometry (Figure 6). Two phases are analyzed in each test case: Phase 1, assimilation window, consisting of 24-hour period with available observation data, and Phase 2, forecast window, consisting of 4-hour model free-run. True state data ("measured" water levels) are synthetically generated using "true inflows" (black line on Fig. 7), while "wrong" inflow (dashed line in Fig. 7) is used to run the model that will be assimilated. True state data are generated using the hydraulic model with the "true inflows". Same initial condition was applied for both assimilation methods tested.

CASE 1 – Channel with rectangular cross section. *50km* long and *250m* wide rectangular channel with longitudinal slope of *1‰*. Manning's roughness used in this test case is uniform $n = 0.03\ m^{-1/3}s$. Spatial resolution is Δx*=125 m* and temporal resolution is Δt*=5 s*ec according to CFL stability condition (Abbot and Basco 1989). Upstream boundary condition is given by the inflow hydrograph (Fig. 7) and normal depth is applied at downstream boundary condition. Bottom level at the upstream boundary is set to 100 m. Six observation points are

used. Three points are used for direct water level assimilation, and the other three points are used for validation (Fig. 6). In order to represent real problem, time step used for observed data collection $\Delta t_{obs}=60s$ is 12 times larger than simulation time step. Standard deviation used for observation uncertainty evaluation is set to 1 cm (this uncertainty is used to represent noise in observation data).

CASE 2 – Channel with compound cross section. *100 km* long compound channel with longitudinal slope of *1‰*. Manning's roughness is not uniform in cross section: the main channel is $n_{mc}=0.018\ m^{-1/3}s$, left floodplain $n_{lfp}=0.025\ m^{-1/3}s$ and $n_{rfp}=0.03\ m^{-1/3}s$ for the right floodplain. Spatial resolution is $\Delta x=250\ m$ and temporal is $\Delta t=10$ *sec* according to CFL stability condition (Abbot and Basco 1989). Upstream boundary condition is given by the inflow hydrograph (Fig. 7) and normal depth is applied at downstream boundary condition. Bottom level at the upstream boundary is set to 100 m. As in CASE 1, six observation points are used, three for assimilation and three for validation (Fig. 6). Observations are generated with time step $\Delta t_{obs}=60\ s$, with standard deviation of uncertainty 1 cm.

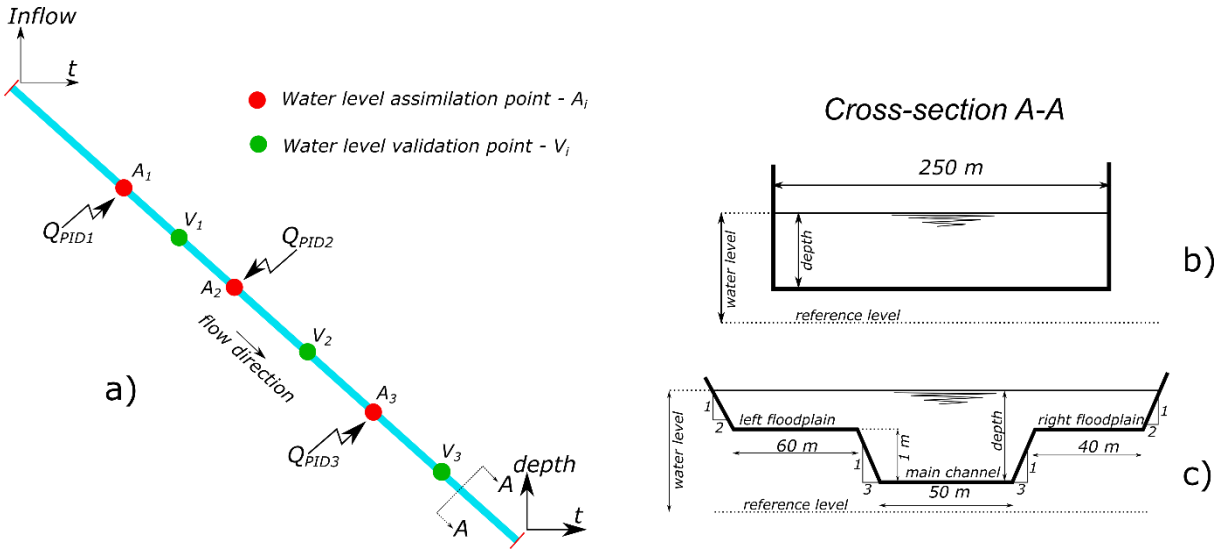

Figure 6. Test cases: a) river section used for data assimilation methods benchmarking; b) rectangular cross-section – **CASE 1**; c) compound channel – **CASE 2**

In both test cases, with rectangular and compound channels, length scale c, eq. (16), used in correlation matrix ρ, is set to 250 m. This value is determined by trial and error in order to determine the minimum value that provides model stability. This shows that correction of water level at assimilation point directly affects water levels in the cross-sections 250 m

upstream and downstream. In other words, two upstream and two downstream sections are affected by water level update at assimilation point in Case 1 (rectangular channel) and one upstream and downstream cross-section in Case 2 (compound channel).

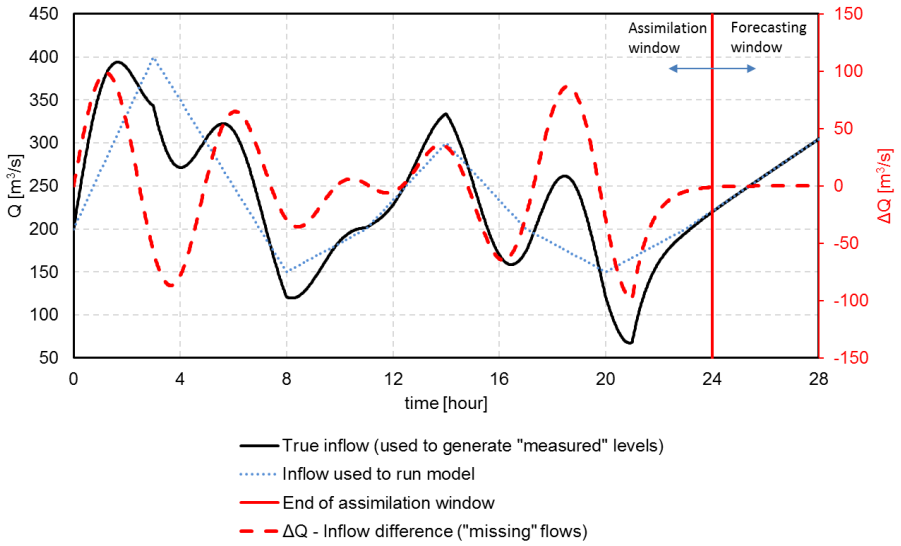

Figure 7. River section inflow for true state generator and inflow for assimilation/forecast

Table 1. Test cases for rectangular and compound channel (Derivative gain D=0 for all cases)

Case		Model	Assimilation method	P	I	Ensemble size
Rectangular	Compound					
R1	*C1*	*DiffW1D*	*PID*	*10*	*0*	*/*
R2	*C2*	*DiffW1D*	*PID*	*10*	*0.1*	*/*
R3	*C3*	*DiffW1D*	*PID*	*10*	*1*	*/*
R4	*C4*	*DiffW1D*	*EnKF*	*/*	*/*	*50*
R5	*C5*	*DiffW1D*	*EnKF*	*/*	*/*	*100*
R6	*C6*	*DiffW1D*	*EnKF*	*/*	*/*	*200*

Different test cases are analyzed regarding P and I gains (D gain was set to 0 in all cases) in PID controller and ensemble size used in EnKF assimilation method (Table 1). Each test case is named according to the following abbreviation *TypeOfCh_AssimMethod* (*TypeOfCh* – *R* for rectangular, *C* for compound; *AssimMethod* – 1 for PI where I=0, 2 for PI where I=0.1, 3 for PI where I=1, 4 for EnKF with 50 ensemble members, 5 for EnKF with 100 ensemble members, 6 for EnKF with 200 ensemble members).

2.5. Assessment methods

Root-mean-square-error (RMSE) is used for assessment of the PID-DA and EnKF data assimilation. RMSE, eq. (20), is calculated according to true state for assimilation window and forecasting window. Besides RMSE, computational time for both assimilation methods is obtained and compared.

$$RMSE = \sqrt{\frac{\sum_{i=1}^{N}\left(X_{sim,i} - X_{true\_state,i}\right)^2}{N}} \tag{20}$$

In eq. (20) X can be water level or discharge obtained by model simulation. Index sim is used for model results using data assimilation and index $true\_state$ is used for true levels or discharges (black line in Fig. 7). N is the number of time steps where both simulation data and observed data are available. As the model/assimilation performance indicator, mean RMSE value for assimilation points and mean RMSE value for validation points is used.

PID-DA and EnKF are also compared regarding runtime and speed up gain. Speed up gain represents the ratio between simulation runtime when EnKF is used and simulation runtime when PID-DA is used, showing how many times the PID-DA simulation is faster than EnKF.

3. RESULTS AND DISCUSSION

All performance indicators, for all test cases defined in Table 1. are presented in Table 2 (rectangular channel) and in Table 3. (compound channel). Beside the above-mentioned tables, RMSE indicators are presented in Figure 8. (rectangular channel) and in Figure 9. (compound channel).

Table 2. Statistical evaluation of the assimilation/forecast (***RMSE$_{assim}$ / RMSE$_{fcst}$***) process – rectangular channel

Case	Mean RMSE - assimilation points	Mean RMSE - validation points	Runtime [sec]
R1	0.069/0.069	0.06/0.084	14.582
R2	0.058/0.084	0.053/0.074	14.612
R3	0.009/0.062	0.012/0.048	14.668
R4	0.092/0.025	0.116/0.026	272.517
R5	0.126/0.025	0.148/0.026	482.489
R6	0.045/0.025	0.044/0.026	920.979

Table 3. Statistical evaluation of the assimilation/forecast (***RMSE$_{assim}$ / RMSE$_{fcst}$***) process – compound channel

Case	Mean RMSE - assimilation points	Mean RMSE - validation points	Runtime [sec]
C1	0.076/0.094	0.07/0.078	9.802
C2	0.061/0.09	0.058/0.07	9.786
C3	0.01/0.059	0.015/0.045	9.779
C4	0.068/0.073	0.08/0.051	188.137
C5	0.031/0.07	0.046/0.049	322.894
C6	0.096/0.079	0.114/0.057	619.648

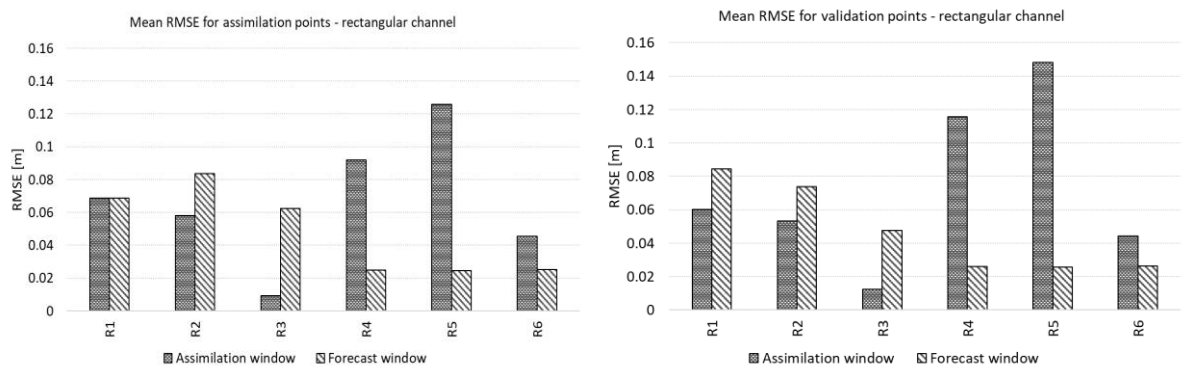

a) b)

Figure 8. RMSE model/assimilation performance indicators for rectangular channel: a) mean statistics for assimilation points (A1, A2, and A3); b) mean statistics for validation points (V1, V2 and V3)

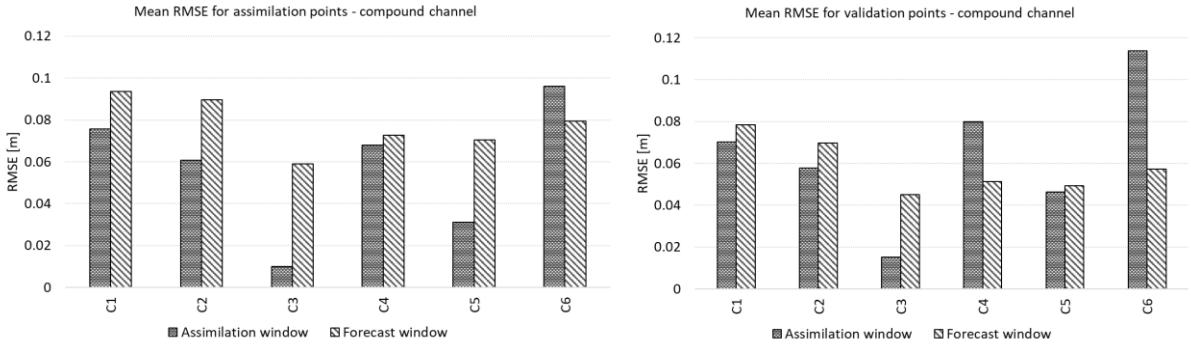

a) b)

Figure 9. RMSE model/assimilation performance indicators for compound channel: a) mean statistics for assimilation points (A1, A2, and A3); b) mean statistics for validation points (V1, V2 and V3)

3.1. Tuning the PID controllers

The *P* and *I* gains in PID controllers could be a matter of separate optimization. In this paper all controllers have the same *P*=10 gain, selected by trial, and *I* gain was tested in the range [0, 0.1 and 1] to present its influence. Figure 10. represents water levels at three assimilation points (A1, A2 and A3 in Fig. 6a) and three validation points (V1, V2 and V3 at Fig. 6a), for

cases C1, C2 and C3. Usage of P gain only in PID controller (*I*=0, case C1) shows the inability of the model to reach the setpoint (measured water levels) during the assimilation (Figure 10). Therefore, integrative gain in PID controllers has to be used. Improvement of assimilation process is visible in cases C2 and R2, where *I* gain is set to 0.1, reducing the mean RMSE value in the assimilation window from 0.069m (for assimilation points) to 0.058m for rectangular channel (Figure 8a), and from 0.06m to 0.053m for validation points (Figure 8b). In cases with compound channel (C1 and C2), mean RMSE for assimilation points drops from 0.076m to 0.061m for assimilation points (Figure 9a), and from 0.07m to 0.058 for validation points (Figure 9b). Increasing the *I* gain by an order of magnitude, to *I*=1 (cases R3 and C3) results in further improvement of visual agreement between modelled and true state and mean RMSE value. In these cases (R3 and C3), mean RMSE value is 0.009m in assimilation window for assimilation points and 0.012m for validation points (rectangular channel, Table 2. and Figure 8), while these values are 0.01m for assimilation points and 0.015m for validation points for compound channel (Table 3. and Figure 9). RMSE value for forecasting window is also reduced from 0.069m in case R1 and 0.084m in case R2 to 0.061m in case R3, at assimilation points. RMSE values are also reduced at validation points, from 0.084m and 0.074m (Cases R1 and R2, respectively) to 0.048m in case R3. For compound channel RMSE values drop from 0.094m (Case C1) and 0.09m (Case C2) to 0.059m (Case C3) at assimilation points, and from 0.078m (Case C1) and 0.07m (Case C2) to 0.045m (Case C3) at validation points.

Further increase of *I* gain (10, 100) shows the increase in instability, big oscillations in correction flows with high amplitude preventing the models to obtain physically sound values for water levels (negative values are obtained; not presented here). In addition, increasing the P gain will also cause the instability (oscillations with high amplitude). Therefore, further analysis of the PID-DA will consider the minimal stable gain settings of *P*=10 and *I*=1.

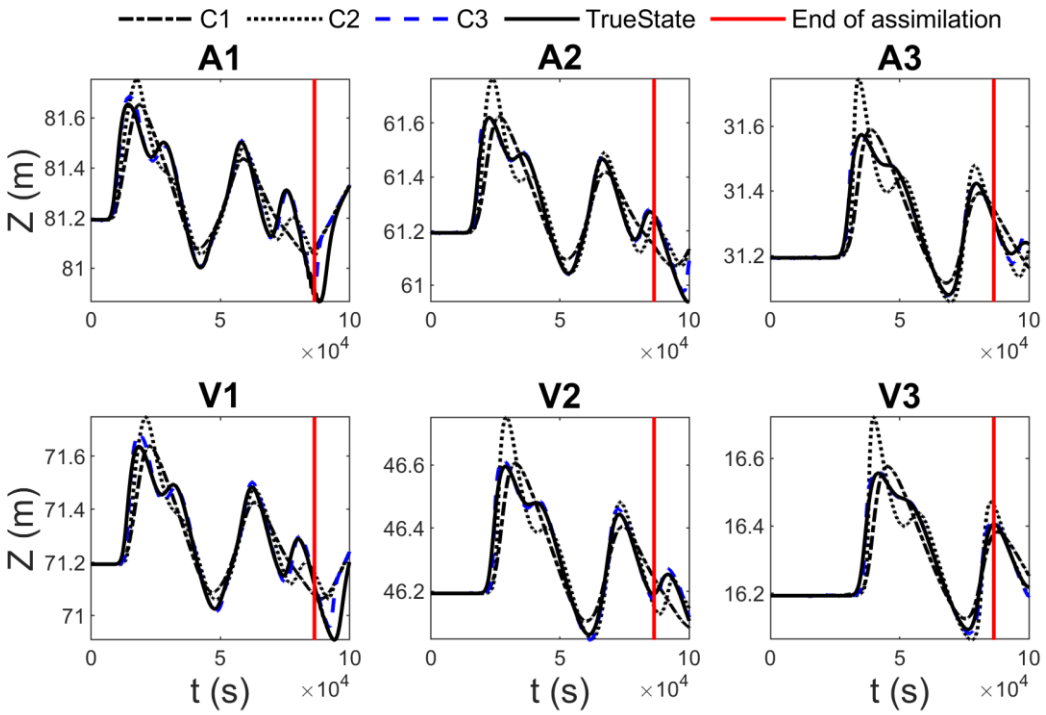

Figure 10. Results of PID control-based data assimilation with different P and I gains

3.2. Correction flows added/subtracted by PID controllers at assimilation points

Figure 11. shows correction flows added/subtracted at assimilation points (upper flow hydrographs are for rectangular channel and lower are for compound channel). In both cases (with rectangular and compound channels) results show that PID controller used to add correction flows at assimilation point A1 provides the most part of the "missing" flows (difference between true inflow and inflow used to run the model, Fig. 7). Max value of correction flow added at A1 (for rectangular channel) is about 84 m^3/s while max value of correction flow subtracted at A1 is approximately 80 m^3/s (correction flow is -80 m^3/s). At assimilation point A2, max value of correction flows are 36 m^3/s and -25 m^3/s, and at assimilation point A3 these values are 25 m^3/s and -22 m^3/s.

When compound channel is analyzed (Fig. 11b), the correction flows slightly differs. At assimilation point A1, max values of correction flows are 82 m^3/s and -65 m^3/s. At assimilation points A2 these values are 25m^3/s and -25m^3/s. At assimilation point A3, correction flows are between 20 m^3/s and -20 m^3/s.

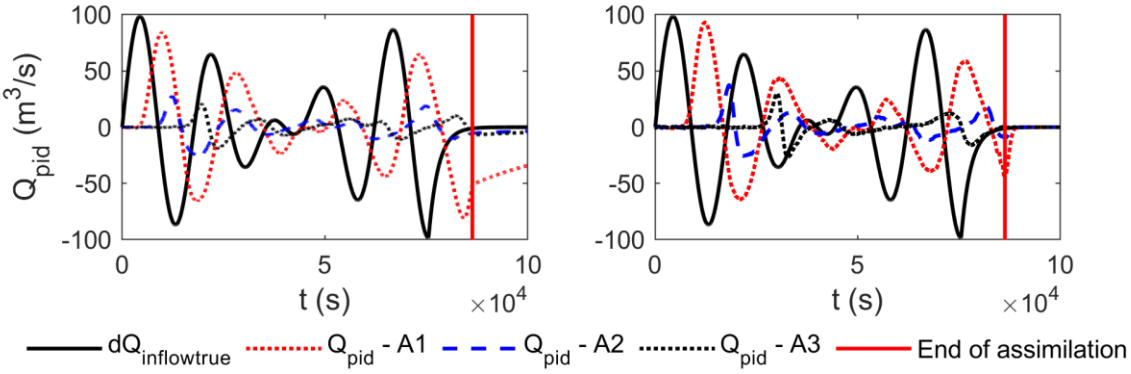

a) b)

Figure 11. Correction flow added/subtracted at assimilation points for: a) rectangular channel b) compound channel

Comparing the correction flow hydrographs, especially for assimilation point A1 (for both channel geometry types) in Figure 11. and "missing" flow hydrograph (flow hydrograph representing the difference between true inflow and inflow used to run the model, red dashed line in Fig. 7.) shows that PID controllers are capable to estimate the true inflow considering flow hydrograph shape and total volume. Correction flow hydrographs are slightly delayed and mitigated due to system dynamics (friction and minor energy losses over the channels).

3.3. EnKF assimilation

Figure 12. shows water levels obtained using coupled DiffW1D model and EnKF assimilation method, with different sizes of ensemble members used to represent model states. Three values for ensemble size are analyzed, 50 (R4 and C4), 100 (R5 and C5) and 200 (R6 and C6). The best results of assimilation process are obtained with 200 ensemble members (Figure 8) for rectangular channel and with 100 ensemble members when compound channel is analyzed. RMSE values for rectangular channel (Table 2.) are 0.045m in assimilation window, at assimilation points, and 0.044m for validation points (for rectangular channel).

Increasing the number of ensemble members doesn't always provide better results in assimilation window. Because there, still, hasn't been determined universal procedure to determine optimal ensemble size in EnKF, different ensemble sizes can sometimes produce

good results. For example, Yin et al. (2015) tested different ensemble sizes in soil moisture data assimilation and showed that large ensemble size doesn't always produce better results.

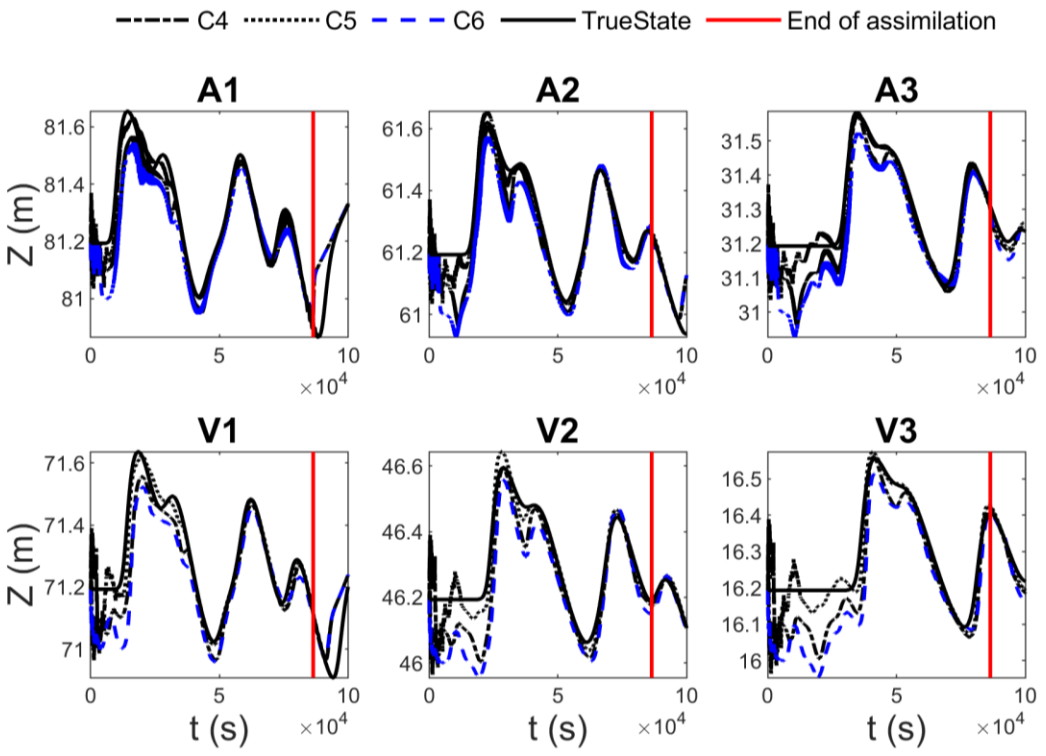

Figure 12. Assimilated water levels using EnKF for different number of ensemble members

3.4. PID-DA and EnKF comparison

Presented tests of the PID-DA (subsections 3.1 and 3.2) and EnKF (subsection 3.3) show that both methods are able to "reach" the true state and give similar results in forecasting window. Looking into the Figure 8, when PID-DA and EnKF are compared on rectangular channel and in assimilation window, it is obvious that PID-DA (when it is properly tuned) shows significantly better results in RMSE statistics. When PID-DA is coupled with DiffW1D model, RMSE for assimilation points is 0.009m, and 0.012m for validation points. On the other hand, coupling hydraulic model with EnKF provides RMSE of 0.045m for assimilation points and 0.044m for validation points (both for rectangular channel). Comparing the results of PID-DA (when controllers are properly tuned, case R3) and EnKF data assimilation

procedure shows that RMSE statistics obtained using PID-DA approach are at least 4 times smaller than results obtained using EnKF approach. This can be seen at Figure 8. when case R3 (which assumes proper tuning of the PID controller's gains) is compared with case R6, when EnKF approach with 200 ensemble members are used. This ratio goes up to 12 times in favor of PID-DA approach when cases R3 and R5 are compared. Similar trend can be seen when RMSE statistics for validation points are compared. Best RMSE value when PID-DA approach is used is obtained for case R3, 0.012m. When EnKF approach is used, best result is obtained using 200 ensemble members (case R6), 0.044m. Comparison of this RMSE values shows that PID-DA approach shows, again, at least 4 times smaller values of RMSE. Comparing case R3 with R5, it can be seen that this ratio, also, goes up to 12 times in favor of PID-DA.

When compound channel is analyzed, PID-DA also shows better results in RMSE statistics than EnKF (Table 3. And Figure 9.). For example, the best results when EnKF is applied are in case C5, where EnKF is used. Comparing these results with the appropriate case when PID-DA is used (case C3), shows that RMSE in this case is almost three times smaller, 0.007m, in the favor of PID-DA. Further looking into the Table 3., containing RMSE statistics for each case tested in this research, and, also, in Figure 9. shows that application of PID-DA methodology provides at least three time better RMSE values (comparing cases C3 and C5) in the assimilation process (assimilation window), while this ratio goes up to 10 times (e.g. when cases C3 and C6 are compared) in the favor of PID-DA.

Main reason for this (for both channel types) is struggling of the EnKF method to reach true state in first couple of hours of assimilation window, as it can be seen in Fig. 13, and in higher RMSE values (Tables 2. and 3. And Figures 8. and 9.), even though the same initial condition is applied for both assimilation methods. The reason for this could be found in the nature of EnKF algorithm (and other standard assimilation methods in general) and its necessity to estimate model uncertainty, unlike PID-DA. Model uncertainty in EnKF is estimated using water levels perturbations. This can cause significant oscillations of the model in early stages of the assimilation window.

On the other hand, PID-DA algorithm skips model uncertainty estimation, which allows reaching the true state much faster than EnKF, but under the assumption that observation uncertainty is much lower than model uncertainty. Using PID-DA, modeled water level will closely follow the observed one, regardless of model nor observed uncertainties, unlike EnKF algorithm, which has the ability to avoid these problems by weighting model and observation uncertainties. In other words, if observed data is with high uncertainty, higher than model's uncertainty, EnKF will give more trust to model than observations, and try to void the observations to a certain extent.

In order to use the PID-DA, it is essential to have observed water levels with high accuracy, which is possible to achieve with contemporary measurement techniques. Additionally, reduction of level measurements of low quality requires the pre-processing phase for data quality estimation (as it is mentioned at the end of section 2.3.1.).

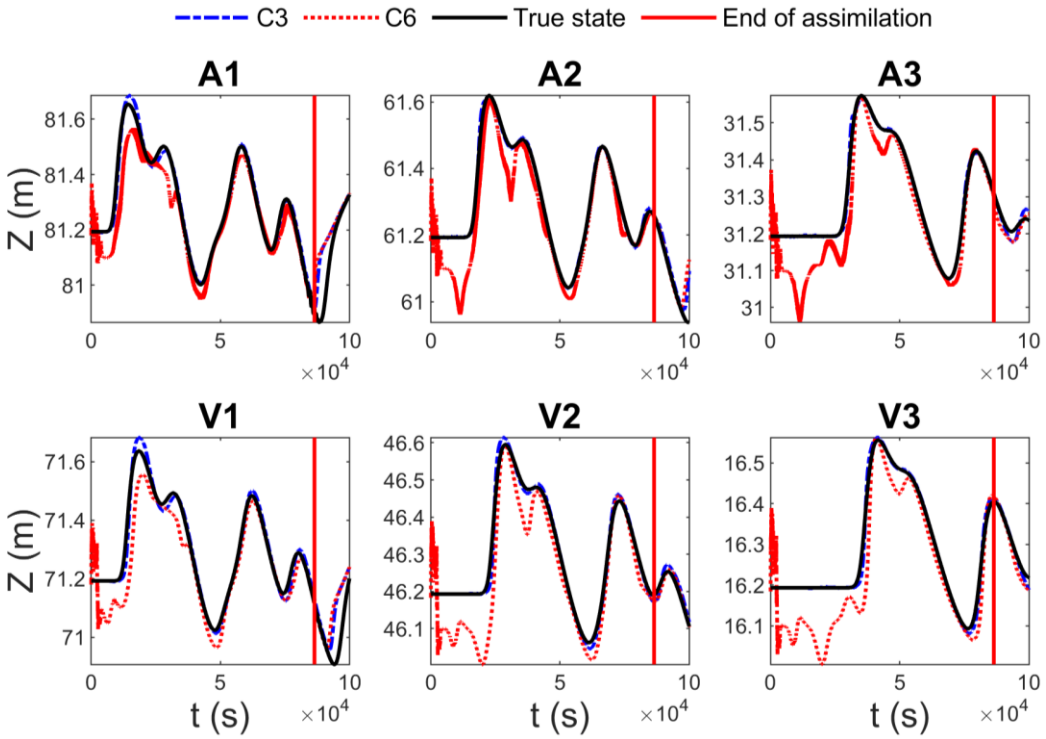

Figure 13. Comparison of assimilated water levels using PID-DA (blue dashed line) and EnKF (red dotted line)

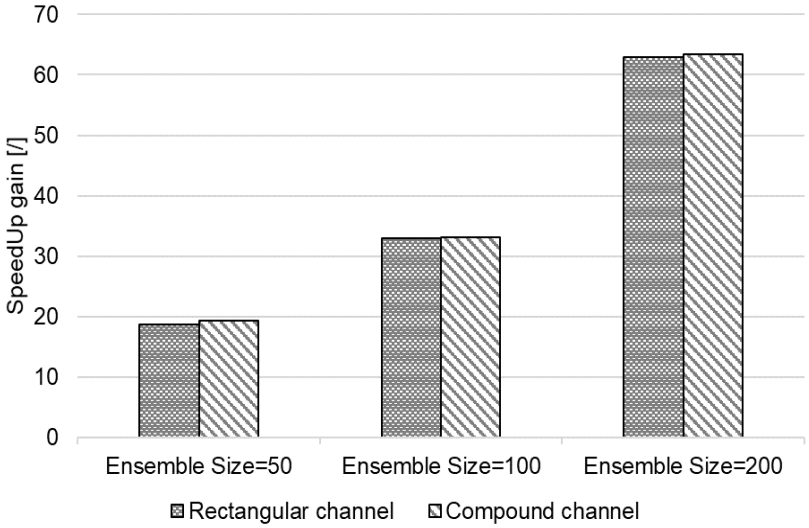

Figure 14. PID-DA speed up gain compared to EnKF with different ensemble size application

Fig. 14 shows average speed up gains (based on the runtimes in Tables 2. and 3.) of the assimilation/forecast process when PID-DA is used as data assimilation method instead of EnKF. Average runtime of assimilations using PID-DA is compared to runtimes when EnKF is applied, with various ensemble sizes. Changing the PID controller's parameters (*P* and *I* gains) or inclusion of error dumping doesn't change the runtime of the assimilation process. However, used ensemble size in EnKF algorithm significantly affects the computational time. Therefore, speed up gain when PID-DA is used increases, compared to EnKF, with increasing the number of ensemble members (Fig. 14). Speed up gain when optimal configuration of PID controllers (outlined in the section 3.1) is used and compared with EnKF with 50 ensemble members is 18.64 for rectangular channel and 19.26 for compound channel. Increasing the size of the ensemble used in EnKF increases the speed up gain, which goes up to 63 for rectangular channel (EnKF with 200 ensemble members) and up to 63.45 for compound channel.

All these results show high potential for application of the PID-DA methodology in 1D open channel models. Nevertheless, it has to be underlined that this type of data assimilation is problem specific, narrowing the application area (only for 1D open channel models, for now). On the other hand, even though this paper shows some advantages of PID-DA (assimilation

speed up), EnKF still has wider applicability area, for different problems, with small modifications, especially when model parameters (e.g. roughness) are corrected along with model state variables (e.g. water levels and/or discharges).

4. Conclusions

This paper presents the novel data assimilation approach (PID-DA) based on a control loop feedback mechanism, applied to 1D hydrodynamic modelling problems. This assimilation tool, applied as a simple lateral inflow element in 1D hydrodynamic model and controlled by PID controller, is compared to widely used data assimilation EnKF method. Both methods are applied on two hypothetical test cases, rivers with rectangular and compound cross sections. Different test cases are created by analyzing the impact of various PID control parameters (Proportional and Integrative gain, without Derivative gain). Along with these test cases, few numerical cases are created and analyzed by changing number of ensemble members in EnKF application. Results are presented in the form of water level time series at several points (three used for direct assimilation, three used for validation). All results, presented for both assimilation methods on two types of channel's geometry, show that data assimilation/forecast in 1D hydraulic modelling can be adequately solved with standard assimilation tools, such as EnKF, but also can be solved more efficiently using simplified methods as PID-DA. This is especially important for large 1D full-scale models, with more than few hundred cross sections, when there is necessity to reduce the simulation/assimilation time. On the other hand, application of the simplified data assimilation algorithms, such as PID-DA, requires additional steps in the pre-processing phase that have to be thoroughly completed before the assimilation process. Analyzing the results through RMSE statistical indicator and speed up gain obtained as a ratio between EnKF runtime and PID control runtime, the following conclusions could be derived:

- Statistical indicator and simulation runtime analysis used for assessment of the assimilation/forecast process shows that, generally, PID controllers can be

adequately implemented as the data assimilation method for faster reaching of the true state of the 1D open channel hydraulic models.

- Speed up gain provided in assimilation/forecast windows using PID controllers significantly rises when ensemble size used in EnKF increases. This is the main benefit of PID-DA. This speeding up is provided by avoiding (or simplification) of the model uncertainty analysis.
- Performance of the PID-DA depends on parameters used in PID controllers. Therefore, pre-processing phase, used for PID controller tuning, is necessary, which is one of the major disadvantages.
- Performance of the PID-DA strongly depends on observation data quality. Because model uncertainty estimation step is omitted when PID controllers are used, this method requires high confidence in observation data. Therefore, additional pre-processing step is required for data quality evaluation of observations. This is also one of PID control application disadvantages.

Based on the results and previous specific conclusions, some general conclusions could be derived. In situations when there is a need for relatively fast simulations and forecasts, simplified data assimilation methods coupled with 1D hydraulic models can be used without significant sacrifice of the accuracy. Hence, usage of the PID controllers as a data assimilation tool shows the potential, especially in short-term simulations and forecasts of water levels. However, some further analysis and investigations are necessary through the application of PID-DA on a real case study. Number of assimilation points (number of PID controllers) and their combined operation, optimal tuning of the PID controller's parameters, together with impact of assimilation window duration have to be analyzed. At the end, the observation data quality assessment in pre-processing phase and inclusion of data uncertainty in PID-DA has to be implemented for full-scale application.

ACKNOWLEDGEMENT

The authors are grateful to the Serbian Ministry of Education, Science and Technological Development for its financial support, project No. TR37010.

References

Abbot, Michael B. and David R. Basco. 1989. *Computational Fluid Dynamics : An Introduction for Engineers*. Harlow, Essex, England : Longman Scientific & Technical ; New York : Wiley.

Anderson, Jeffrey L. 2007. “An Adaptive Covariance Inflation Error Correction Algorithm for Ensemble Filters.” *Tellus, Series A: Dynamic Meteorology and Oceanography* 59(2):210–24.

Anderson, Jeffrey L. and Stephen L. Anderson. 1999. “A Monte Carlo Implementation of the Nonlinear Filtering Problem to Produce Ensemble Assimilations and Forecasts.” *Monthly Weather Review* 127:2741–58.

Andreadis, Konstantinos M., Elizabeth A. Clark, Dennis P. Lettenmaier, and Douglas E. Alsdorf. 2007. “Prospects for River Discharge and Depth Estimation through Assimilation of Swath-Altimetry into a Raster-Based Hydrodynamics Model.” *Geophysical Research Letters* 34(10):1–5.

Andreadis, Konstantinos M. and Guy J. P. Schumann. 2014. “Estimating the Impact of Satellite Observations on the Predictability of Large-Scale Hydraulic Models.” *Advances in Water Resources* 73:44–54.

Bai, Yun, Zhiqiang Chen, Jingjing Xie, and Chuan Li. 2016. “Daily Reservoir Inflow Forecasting Using Multiscale Deep Feature Learning with Hybrid Models.” *Journal of Hydrology* 532:193–206.

Barthélémy, S., S. Ricci, M. C. Rochoux, E. Le Pape, and O. Thual. 2017. “Ensemble-Based Data Assimilation for Operational Flood Forecasting – On the Merits of State Estimation for 1D Hydrodynamic Forecasting through the Example of the ‘Adour Maritime’ River.” *Journal of Hydrology* 552:210–24.

Bates, P. D. and A. P. J. De Roo. 2000. “A Simple Raster-Based Model for Flood Inundation Simulation.” 236:54–77.

Bozzi, Silvia, Giuseppe Passoni, Pietro Bernardara, Nicole Goutal, and Aurélie Arnaud. 2015. “Roughness and Discharge Uncertainty in 1D Water Level Calculations.” *Environmental Modeling and Assessment* 20(4):343–53.

Brandimarte, Luigia and Giuliano Di Baldassarre. 2012. “Uncertainty in Design Flood Profiles Derived by Hydraulic Modelling.” *Hydrology Research* 43(6):753–61.

Branisavljević, N., D. Prodanović, and D. Pavlović. 2010. “Automatic, Semi-Automatic and Manual Validation of

621 Urban Drainage Data." *Water Science and Technology* 62(5):1013–21.

622 Branisavljević, Nemanja, Zoran Kapelan, and Dušan Prodanović. 2011. "Improved Real-Time Data Anomaly
623 Detection Using Context Classification." *Journal of Hydroinformatics* 13(3):307.

624 Brunner, Gary W. 2010. "HEC-RAS River Analysis System Hydraulic Reference Manual."

625 Chen, Minghong, Juanjuan Pang, and Pengxiang Wu. 2018. "Flood Routing Model with Particle Filter-Based Data
626 Assimilation for Flash Flood Forecasting in the Micro-Model of Lower Yellow River, China." *Water*
627 *(Switzerland)* 10(11).

628 Clark, Martyn P., David E. Rupp, Ross A. Woods, Xiaogu Zheng, Richard P. Ibbitt, Andrew G. Slater, Jochen
629 Schmidt, and Michael J. Uddstrom. 2008. "Hydrological Data Assimilation with the Ensemble Kalman Filter:
630 Use of Streamflow Observations to Update States in a Distributed Hydrological Model." *Advances in Water*
631 *Resources* 31(10):1309–24.

632 Cooper, E. S., S. L. Dance, J. Garcia-Pintado, N. K. Nichols, and P. J. Smith. 2018. "Observation Impact, Domain
633 Length and Parameter Estimation in Data Assimilation for Flood Forecasting." *Environmental Modelling and*
634 *Software* 104:199–214.

635 Costabile, Pierfranco and Francesco Macchione. 2012. "Analysis of One-Dimensional Modelling for Flood Routing
636 in Compound Channels." *Water Resources Management* 26(5):1065–87.

637 Coumou, Dim and Stefan Rahmstorf. 2012. "A Decade of Weather Extremes." *Nature Climate Change* 2(7):491–
638 96.

639 Evensen, Geir. 1994. "Sequential Data Assimilation with a Nonlinear Quasi-Geostrophic Model Using Monte Carlo
640 Methods to Forecast Error Statistics." *Journal of Geophysical Research* 99(C5):10143.

641 Evensen, Geir. 2003. "The Ensemble Kalman Filter: Theoretical Formulation and Practical Implementation."
642 *Ocean Dynamics* 53(4):343–67.

643 García-Pintado, Javier, Jeff C. Neal, David C. Mason, Sarah L. Dance, and Paul D. Bates. 2013. "Scheduling
644 Satellite-Based SAR Acquisition for Sequential Assimilation of Water Level Observations into Flood
645 Modelling." *Journal of Hydrology* 495:252–66.

646 Gaspari, Gregory and Stephen E. Cohn. 1999. "Construction of Correlation Functions in Two and Three
647 Dimensions." *Quarterly Journal of the Royal Meteorological Society* 125(April 1998):723–57.

648 Goutal, N. and F. Maurel. 2002. "A Finite Volume Solver for 1D Shallow Water Equations Applies to an Actual
649 River." *Int. J. Numer. Meth. Fluids* 19(January 2001):1–19.

650 Habert, J., S. Ricci, E. Le Pape, O. Thual, A. Piacentini, N. Goutal, G. Jonville, and M. Rochoux. 2016. "Reduction

of the Uncertainties in the Water Level-Discharge Relation of a 1D Hydraulic Model in the Context of Operational Flood Forecasting." *Journal of Hydrology* 532:52–64.

Hamill, Thomas M., Jeffrey S. Whitaker, and Chris Snyder. 2001. "Distance-Dependent Filtering of Background Error Covariance Estimates in an Ensemble Kalman Filter." *Monthly Weather Review* 129(11):2776–90.

Hansen, Lisbet Sneftrup, Morten Borup, Arne Møller, and Peter Steen Mikkelsen. 2014. "Flow Forecasting Using Deterministic Updating of Water Levels in Distributed Hydrodynamic Urban Drainage Models." *Water (Switzerland)* 6(8):2195–2211.

IPCC. 2012. *Managing the Risks of Extreme Events and Disasters to Advance Climate Change Adaptation*. The Edinburgh Building, Shaftesbury Road, Cambridge CB2 8RU ENGLAND.

Jean-Baptiste, Nelly, Pierre Olivier Malaterre, Christophe Dorée, and Jacques Sau. 2011. "Data Assimilation for Real-Time Estimation of Hydraulic States and Unmeasured Perturbations in a 1D Hydrodynamic Model." *Mathematics and Computers in Simulation* 81(10):2201–14.

Kabir, Sk Faisal, Godwin Appiah Assumaning, and Shoou Yuh Chang. 2017. "Efficiency of Using 4DVar, 3DVar and EnKF Data Assimilation Methods in Groundwater Contaminant Transport Modelling." *European Journal of Environmental and Civil Engineering* 8189(August):1–17.

Kalman, R. E. 1960. "A New Approach to Linear Filtering and Prediction Problems." *Journal of Basic Engineering* 82(1):35.

Karl Astrom, Johan. 2002. "PID Control." *Control System Design*.

Li, Liangping, Ryan Puzel, and Arden Davis. 2018. "Data Assimilation in Groundwater Modelling: Ensemble Kalman Filter versus Ensemble Smoothers." *Hydrological Processes* 32(13):2020–29.

Li, Liangping, Larry Stetler, Zhendan Cao, and Arden Davis. 2018. "An Iterative Normal-Score Ensemble Smoother for Dealing with Non-Gaussianity in Data Assimilation." *Journal of Hydrology* (January).

Madsen, Henrik, Johan Hartnack, and Jacob V. T. Sørensen. 2006. "Data Assimilation in a Flood Modelling System Using the Ensemble Kalman Filter." *XVI International Conference on Computational Methods in Water Resources (CMWR-XVI)* 16:1–8.

Madsen, Henrik, Dan Rosbjerg, Jesper Damgàrd, &. Frands, and S0bjerg Hansen. 2003. "Data Assimilation in the MIKE 11 Flood Forecasting System Using Kalman Filtering." *Water Resources Systems— Hydrological Risk, Management and Development* (281):75–81.

Madsen, Henrik and Claus Skotner. 2005. "Adaptive State Updating in Real-Time River Flow Forecasting - A Combined Filtering and Error Forecasting Procedure." *Journal of Hydrology* 308(1–4):302–12.

Mason, D. C., G. J. P. Schumann, J. C. Neal, J. Garcia-Pintado, and P. D. Bates. 2012. “Automatic near Real-Time Selection of Flood Water Levels from High Resolution Synthetic Aperture Radar Images for Assimilation into Hydraulic Models: A Case Study.” *Remote Sensing of Environment* 124:705–16.

Matgen, P., M. Montanari, R. Hostache, L. Pfister, L. Hoffmann, D. Plaza, V. R. N. Pauwels, G. J. M. De Lannoy, R. De Keyser, and H. H. G. Savenije. 2010. “Towards the Sequential Assimilation of SAR-Derived Water Stages into Hydraulic Models Using the Particle Filter: Proof of Concept.” *Hydrology and Earth System Sciences* 14(9):1773–85.

MathWorks Inc. 2015. “MATLAB Version 8.6. 0.267246 (R2018b).”

Milasinovic, Milos, Budo Zindovic, Nikola Rosic, and Dusan Prodanovic. 2019. “PID Controllers as Data Assimilation Tool for 1D Hydrodynamic Models of Different Complexity.” in *Proceedings of the 5th International conference SimHydro 2019*. Nice.

Milasinovic, Milos, Budo Zindovic, Nikola Rosic, and Dušan Prodanović. 2018. “ANALYSIS OF THE 1D HYDRODYNAMIC MODEL COMPLEXITY INFLUENCE ON PID CONTROLLER BASED DATA ASSIMILATION – PRELIMINARY RESULTS: In Serbian.” *Vodoprivreda* 50:245–54.

Moradkhani, Hamid, Kuo-Lin Hsu, Hoshin Gupta, and Soroosh Sorooshian. 2005. “Uncertainty Assessment of Hydrologic Model States and Parameters: Sequential Data Assimilation Using the Particle Filter.” *Water Resources Research* 41(5):1–17.

Del Moral, Pierre. 1997. “Nonlinear Interacting Filtering : Particle.” *Comptes Rendus de l’Académie Des Sciences - Series I - Mathematics* 325(1):653–58.

Munier, S., A. Polebitski, C. Brown, G. Belaud, and D. P. Lettenmaier. 2014. “SWOT Data Assimilation for Operational Reservoir Management on the Upper Niger River Basin.” *Water Resources Research* 51:554–75.

Neal, Jeffrey C., Peter M. Atkinson, and Craig W. Hutton. 2007. “Flood Inundation Model Updating Using an Ensemble Kalman Filter and Spatially Distributed Measurements.” *Journal of Hydrology* 336(3–4):401–15.

Neal, Jeffrey, Guy Schumann, Paul Bates, Wouter Buytaert, Patrick Matgen, and Florian Pappenberger. 2009. “A Data Assimilation Approach to Discharge Estimation from Space.” *Hydrological Processes* 23:3641–49.

Ocio, David, Nataliya Le Vine, Ida Westerberg, Florian Pappenberger, and Wouter Buytaert. 2017. “The Role of Rating Curve Uncertainty in Real-Time Flood Forecasting.” *Water Resources Research* 53(5):4197–4213.

Petrie, Ruth E. and Sarah L. Dance. 2010. “Ensemble-Based Data Assimilation and the Localisation Problem.” *Weather* 65(3):65–69.

711 Petrovic, Jasna, Bojan Palmar, and Marko Ivetic. 1994. “Transformacija Poplavnog Talasa Metodom Razdvajanja
712 Operatora: In Serbian.” Pp. 145–50 in *Zbornik radova 11. savetovanja JDHI i JDH*. Belgrade.

713 Reichle, Rolf H., Jeffrey P. Walker, Randal D. Koster, and Paul R. Houser. 2002. “Extended versus Ensemble
714 Kalman Filtering for Land Data Assimilation.” *Journal of Hydrometeorology* 3(6):728–40.

715 Rosić, Nikola, Nenad Jaćimović, Dušan Prodanović, and Boban Stojanović. 2017. “Data Assimilation for
716 Operational Reservoir Management on the Danube River.” *7th International Conference on Information*
717 *Society and Technology ICIST 2017* 210–13.

718 Rosić, Nikola, Dušan Prodanović, Boban Stojanović, and Dragana Obradović. 2017. “NEAR REAL TIME DATA
719 ASSIMILATION OF NUMERICAL SIMULATION MODEL FOR DANUBE RIVER FROM NOVI SAD TO
720 IRON GATE I, TEST RESULTS: In Serbian.” *Vodoprivreda* 49(288):253–61.

721 Schütze, Manfred, Alberto Campisano, Hubert Colas, Wolfgang Schilling, and Peter A. Vanrolleghem. 2004. “Real
722 Time Control of Urban Wastewater Systems - Where Do We Stand Today?” *Journal of Hydrology* 299(3–
723 4):335–48.

724 Seo, Dong Jun, Lee Cajina, Robert Corby, and Tracy Howieson. 2009. “Automatic State Updating for Operational
725 Streamflow Forecasting via Variational Data Assimilation.” *Journal of Hydrology* 367(3–4):255–75.

726 Skogestad, Sigurd. 2004. “Simple Analytic Rules for Model Reduction and PID Controller Tuning.” *Modeling,*
727 *Identification and Control* 25(2):85–120.

728 Todorovic, Andrijana and Jasna Plavsic. 2016. “The Role of Conceptual Hydrologic Model Calibration in Climate
729 Change Impact on Water Resources Assessment.” *Journal of Water and Climate Change* 7(1):16–28.

730 Vrugt, Jasper A., Cajo J. F. ter Braak, Martyn P. Clark, James M. Hyman, and Bruce A. Robinson. 2008.
731 “Treatment of Input Uncertainty in Hydrologic Modeling: Doing Hydrology Backward with Markov Chain
732 Monte Carlo Simulation.” *Water Resources Research* 44(12):1–15.

733 Vrugt, Jasper A., Hoshin V. Gupta, BreanndánÓ Nualláin, and Willem Bouten. 2006. “Real-Time Data
734 Assimilation for Operational Ensemble Streamflow Forecasting.” *Journal of Hydrometeorology* 7(3):548–65.

735 Wang, Bin, Juanjuan Liu, Li Liu, Shiming Xu, and Wenyu Huang. 2018. “An Approach to Localization for
736 Ensemble-Based Data Assimilation.” *PLoS ONE* 13(1):11–26.

737 Wu, Guocan and Xiaogu Zheng. 2018. “The Error Covariance Matrix Inflation in Ensemble Kalman Filter.” *Kalman*
738 *Filters - Theory for Advanced Applications*.

739 Xu, Xingya, Xuesong Zhang, Hongwei Fang, Ruixun Lai, Yuefeng Zhang, Lei Huang, and Xiaobo Liu. 2017. “A
740 Real-Time Probabilistic Channel Flood-Forecasting Model Based on the Bayesian Particle Filter Approach.”

741 *Environmental Modelling and Software* 88:151–67.

742 Yen, Ben Chie. 2002. “Open Channel Flow Resistance.” *Journal of Hydraulic Engineering* 128(1):20–39.

743 Yin, Jifu, Xiwu Zhan, Youfei Zheng, Christopher R. Hain, Jicheng Liu, and Li Fang. 2015. “Optimal Ensemble Size
744 of Ensemble Kalman Filter in Sequential Soil Moisture Data Assimilation.” *Geophysical Research Letters*
745 42(16):6710–15.

746 Ziegler, J. G. and N. B. Nichols. 1995. “Optimum Settings for Automatic Controllers.” *InTech* 42(6):94–100.